

The Exponential Transformation Based Lattice Boltzmann Model for Convection-Diffusion Equation

Ting Zhang¹, Shuqi Cui^{2,*}, Ning Hong² and Baochang Shi^{3,4}

¹ College of Sciences, Wuhan University of Science and Technology, Wuhan, Hubei 430081, China

² School of General Education, Wuchang University of Technology, Wuhan, Hubei 430223, China

³ Institute of Interdisciplinary Research for Mathematics and Applied Science, School of Mathematics and Statistics, Huazhong University of Science and Technology, Wuhan, Hubei 430074, China

⁴ Hubei Key Laboratory of Engineering Modeling and Scientific Computing, Huazhong University of Science and Technology, Wuhan, Hubei 430074, China

Received 20 January 2023; Accepted (in revised version) 4 August 2023

Abstract. In this paper, an exponential transformation based lattice Boltzmann (LB) model for solving the n -dimensional (nD) convection-diffusion equation (CDE) is developed. Firstly, a class of exponential transformation is proposed to convert the nD CDE into a diffusion equation. Then, the converted diffusion equation is solved by the LB model. So, compared to the available LB models for CDE, the present LB model can eliminate the difficulty in treating the convection term. With the direct Taylor expansion method, it is shown that the CDE can be exactly derived from the exponential transformation based LB model. Finally, a variety of numerical tests have been conducted to validate the present LB model. It can be found that the numerical results agree well with the analytical solutions. Moreover, we also find that the present LB model has second-order convergence rate in space, and it is more effective and more stable than the previous LB model for the CDE.

AMS subject classifications: 76M28, 65N75

Key words: Lattice Boltzmann model, convection-diffusion equation, exponential transformation.

1 Introduction

As an important kind of partial differential equations (PDEs), the convection-diffusion equation (CDE) has gained much attention in the study of complex phenomena in many

*Corresponding author.

Email: csqi2010@126.com (S. Cui)

fields. However, it is usually difficult to obtain the analytical solutions of most of the CDEs. With the development of computing technique, some numerical approaches have been developed to solve the CDE, including the explicit and implicit finite-difference method, finite-element method, finite-volume method, meshless method, and so on [1–8].

The mesoscopic lattice Boltzmann method (LBM) originated from kinetic theory [9–13], has gained much attention in solving nonlinear systems. As an alternative to the traditional numerical methods, the LBM has many advantages for its distinct features, such as the simplicity of programming, locality of computation, and ease in dealing with complex boundaries. In recent years, the LBM has also been successfully applied to solve the Poisson equation, Laplace equation, Burgers' equation, reaction-diffusion equation, CDE, and so on [14–25].

Although many LB models have been proposed for the CDE, there are still some problems. The first is that when the simple linear equilibrium distribution function is used, we need to add an additional source term in the evolution equation to eliminate the effect of the convection term. The second is that if a more complex equilibrium distribution with the quadratic form is applied, a numerical diffusion would be induced. The third is that the convection term usually causes a numerical instability problem in the LBM, and it should be treated properly. Thus, if the convection term in the CDE can be eliminated, the problems inherited in these LB models for the CDE will be overcome.

As early as 1962, Brenner et al. [26] first adopted a transformation to reduce the CDE to a heat conduction equation. In the year of 2013, Zhang et al. [27] introduced a similar exponential transformation to eliminate the convection term in the nonlinear delay convection-reaction-diffusion equations. However, only one-dimensional CDEs were solved in their works. In this paper, the exponential transformation is extended to convert the n -dimensional (nD) CDE into a nD diffusion equation, then a LB method is developed to solve the converted nD diffusion equation. In the exponential transformation based LBM, we can use the simple linear equilibrium distribution function and discrete velocity lattice model, and thus the computation efficiency and stability of the LBM for CDE can be improved.

The rest of the paper is organized as follows. In Section 2, an exponential transformation based LB model for nD CDE is proposed. In Section 3, some numerical simulations are performed to test the present LB model, and finally some conclusions are given in Section 4.

2 Lattice Boltzmann model for convection-diffusion equation

In this section, the nD CDE is first converted into a diffusion equation by the exponential transformation, and then a LB model for the converted diffusion equation is developed.

In this paper, the following nD CDE with a source term is considered,

$$\partial_t \rho + \mathbf{u} \cdot \nabla \rho = \nabla \cdot (\alpha \nabla \rho) + F(\mathbf{x}, t), \quad (2.1)$$

where $\mathbf{u} \cdot \nabla \rho$ is a convection term, ρ is a scalar variable at time t and space \mathbf{x} , $\mathbf{u} = (u_1, u_2, \dots, u_n)^T$ is a constant vector, ∇ is a gradient operator, α is a diffusion coefficient and $F(\mathbf{x}, t)$ is a source term.

The initial condition associated with Eq. (2.1) is given by

$$\rho(\mathbf{x}, 0) = \rho_0(\mathbf{x}), \quad \mathbf{x} \in \Omega, \quad (2.2)$$

where Ω is the domain of \mathbf{x} .

The boundary conditions corresponding to Eq. (2.1) are given by

$$\rho(\tilde{\mathbf{x}}, t) = g(\tilde{\mathbf{x}}, t), \quad 0 \leq t \leq T, \quad \tilde{\mathbf{x}} \in \partial\Omega, \quad (2.3)$$

where $\partial\Omega$ is the boundary of Ω .

Employing the following exponential transformation to Eq. (2.1),

$$\rho(\mathbf{x}, t) = \phi(\mathbf{x}, t) \exp(\mathbf{P} \cdot \mathbf{x} + qt), \quad (2.4)$$

where $\mathbf{P} = (p_1, p_2, \dots, p_n)^T$ is a constant vector and q is a constant scalar variable. We have

$$\begin{aligned} & \exp(\mathbf{P} \cdot \mathbf{x} + qt) (\partial_t \phi + q\phi) + \mathbf{u} \cdot \exp(\mathbf{P} \cdot \mathbf{x} + qt) (\nabla \phi + \mathbf{P}\phi) \\ &= \nabla \cdot \alpha \exp(\mathbf{P} \cdot \mathbf{x} + qt) (\nabla \phi + \mathbf{P}\phi) + F(\mathbf{x}, t), \end{aligned}$$

or, equivalently,

$$\partial_t \phi + (q + \mathbf{u} \cdot \mathbf{P} - \alpha \mathbf{P} \cdot \mathbf{P}) \phi + (\mathbf{u} - 2\alpha \mathbf{P}) \cdot \nabla \phi = \nabla \cdot (\alpha \nabla \phi) + \exp(-\mathbf{P} \cdot \mathbf{x} - qt) F(\mathbf{x}, t).$$

To eliminate the convection term, we let $\mathbf{P} = \frac{\mathbf{u}}{2\alpha}$. For simplicity, we take

$$q = \alpha \mathbf{P} \cdot \mathbf{P} - \mathbf{u} \cdot \mathbf{P} = -\frac{\mathbf{u} \cdot \mathbf{u}}{4\alpha}.$$

Then, the n D CDE (2.1) is converted into the following n D diffusion equation,

$$\partial_t \phi = \nabla \cdot (\alpha \nabla \phi) + G(\mathbf{x}, t), \quad (2.5)$$

where

$$G(\mathbf{x}, t) = \exp(-\mathbf{P} \cdot \mathbf{x} - qt) F(\mathbf{x}, t).$$

Additionally, the initial condition (2.2) and the boundary conditions (2.3) can be written as

$$\phi(\mathbf{x}, 0) = \exp(-\mathbf{P} \cdot \mathbf{x}) \rho_0(\mathbf{x}), \quad \mathbf{x} \in \Omega, \quad (2.6a)$$

$$\phi(\tilde{\mathbf{x}}, t) = \exp(-\mathbf{P} \cdot \tilde{\mathbf{x}} - qt) g(\tilde{\mathbf{x}}, t), \quad 0 \leq t \leq T, \quad \tilde{\mathbf{x}} \in \partial\Omega. \quad (2.6b)$$

Now, we propose a LB model for the diffusion equation (2.5). The evolution equation of the distribution function in the model is

$$f_j(\mathbf{x} + \mathbf{c}_j \Delta t, t + \Delta t) = f_j(\mathbf{x}, t) - \frac{1}{\tau} [f_j(\mathbf{x}, t) - f_j^{eq}(\mathbf{x}, t)] + \Delta t \left[G_j(\mathbf{x}, t) + \frac{\Delta t}{2} \bar{D}_j G_j(\mathbf{x}, t) \right], \quad (2.7)$$

where $f_j(\mathbf{x}, t)$ is the distribution function associated with the discrete velocity \mathbf{c}_j at position \mathbf{x} and time t , Δt is the time step, τ is the dimensionless relaxation time, and $\bar{D}_j = \partial_t + \gamma \mathbf{c}_j \cdot \nabla$ with free parameters $\gamma \in \{0, 1\}$. $\bar{D}_j G_j(x, t)$ can be computed by the following difference schemes [19]:

$$\begin{aligned}\bar{D}_j G_j(x, t) &= (G_j(x, t) - G_j(x, t - \Delta t)) / \Delta t & \text{for } \gamma = 0, \\ \bar{D}_j G_j(x, t) &= (G_j(x, t) - G_j(x - \mathbf{c}_j \Delta t, t - \Delta t)) / \Delta t & \text{for } \gamma = 1.\end{aligned}$$

The local equilibrium distribution function $f_j^{eq}(\mathbf{x}, t)$ is defined by

$$f_j^{eq}(\mathbf{x}, t) = \omega_j \phi, \quad (2.8)$$

where ω_j is the weight coefficient and depends on the lattice model used. Here the DnQ(2n+1) lattice model can be used. For the DnQ(2n+1) lattice model, ω_j can be given as follows:

$$\omega_1 \sim \omega_{2n} = a \quad \text{in} \quad \left(0, \frac{1}{2n}\right], \quad \omega_0 = 1 - 2na.$$

Then the so-called sound speed c_s , which satisfies

$$\sum_j \omega_j \mathbf{c}_j \mathbf{c}_j = c_s^2 \mathbf{I},$$

can be determined by $c_s = \sqrt{2ac}$, where $c = \frac{\Delta x}{\Delta t}$ and Δx is the lattice spacing. $f_j(\mathbf{x}, t)$ and $f_j^{eq}(\mathbf{x}, t)$ satisfy the following equations:

$$\sum_j f_j(\mathbf{x}, t) = \sum_j f_j^{eq}(\mathbf{x}, t) = \phi, \quad \sum_j \mathbf{c}_j f_j^{eq}(\mathbf{x}, t) = 0, \quad \sum_j \mathbf{c}_j \mathbf{c}_j f_j^{eq}(\mathbf{x}, t) = c_s^2 \phi \mathbf{I}. \quad (2.9)$$

It is worth mentioning that, the popular LBM for CDE usually needs the use of the quadratic equilibrium distribution function, or linear equilibrium distribution function and auxiliary source term which is related to the time derivative of the convection term. Besides that, the convection term may cause a numerical instability problem in the LBM. However, the advantages of the LB model for DE are as follows: the equilibrium function is simple, fewer discrete velocities can be adopted (at least $2n$ discrete velocities can be used when $a = \frac{1}{2n}$), and the weight coefficients are flexible.

The source distribution function $G_j(\mathbf{x}, t)$ is given by

$$G_j(\mathbf{x}, t) = \omega_j G, \quad (2.10)$$

which satisfies

$$\sum_j G_j(\mathbf{x}, t) = G, \quad \sum_j \mathbf{c}_j G_j(\mathbf{x}, t) = 0.$$

We now apply the direct Taylor expansion method to derive the converted diffusion equation (2.5). Taking the Taylor series expansion to Eq. (2.7), we can obtain

$$\sum_{i=1}^k \frac{\Delta t^i}{i!} D_j^i f_j + \mathcal{O}(\Delta t^{k+1}) = -\frac{1}{\tau} f_j^{ne} + \Delta t \left(G_j + \frac{\Delta t}{2} \bar{D}_j G_j \right), \quad (2.11)$$

where

$$D_j = \partial_t + \mathbf{c}_j \cdot \nabla \quad \text{and} \quad f_j^{ne} = f_j - f_j^{eq}.$$

From Eq. (2.11), it is easy to get

$$f_j^{ne} = \mathcal{O}(\Delta t). \quad (2.12)$$

With the relation $f_j = f_j^{eq} + f_j^{ne}$ and Eq. (2.12), we can rewrite Eq. (2.11) as

$$\sum_{i=1}^{k-1} \frac{\Delta t^i}{i!} D_j^i (f_j^{eq} + f_j^{ne}) + \frac{\Delta t^k}{k!} D_j^k f_j^{eq} + \mathcal{O}(\Delta t^{k+1}) = -\frac{1}{\tau} f_j^{ne} + \Delta t \left(G_j + \frac{\Delta t}{2} \bar{D}_j G_j \right). \quad (2.13)$$

From Eq. (2.13), the equations at the second and third-orders of Δt can be derived,

$$\Delta t D_j f_j^{eq} = -\frac{1}{\tau} f_j^{ne} + \Delta t G_j + \mathcal{O}(\Delta t^2), \quad (2.14a)$$

$$\Delta t D_j (f_j^{eq} + f_j^{ne}) + \frac{\Delta t^2}{2!} D_j^2 f_j^{eq} = -\frac{1}{\tau} f_j^{ne} + \Delta t \left(G_j + \frac{\Delta t}{2} \bar{D}_j G_j \right) + \mathcal{O}(\Delta t^3), \quad (2.14b)$$

which are equivalent to

$$D_j f_j^{eq} = -\frac{1}{\tau \Delta t} f_j^{ne} + G_j + \mathcal{O}(\Delta t), \quad (2.15a)$$

$$D_j (f_j^{eq} + f_j^{ne}) + \frac{\Delta t}{2!} D_j^2 f_j^{eq} = -\frac{1}{\tau \Delta t} f_j^{ne} + G_j + \frac{\Delta t}{2} \bar{D}_j G_j + \mathcal{O}(\Delta t^2). \quad (2.15b)$$

Multiplying the operator D_j on both sides of Eq. (2.15a), and substituting the result into Eq. (2.15b), we have

$$D_j f_j^{eq} + \left(1 - \frac{1}{2\tau} \right) D_j f_j^{ne} + \frac{\Delta t}{2} D_j G_j = -\frac{1}{\tau \Delta t} f_j^{ne} + G_j + \frac{\Delta t}{2} \bar{D}_j G_j + \mathcal{O}(\Delta t^2). \quad (2.16)$$

Summing Eqs. (2.15a) and (2.16) over j and using Eqs. (2.9), the following equations are obtained,

$$\partial_t \phi = G + \mathcal{O}(\Delta t), \quad (2.17a)$$

$$\partial_t \phi + \left(1 - \frac{1}{2\tau} \right) \nabla \cdot \left(\sum_j \mathbf{c}_j f_j^{ne} \right) = G + \mathcal{O}(\Delta t^2). \quad (2.17b)$$

Based on Eq. (2.15a), we have

$$\sum_j \mathbf{c}_j f_j^{ne} = -\tau \Delta t \left(\sum_j \mathbf{c}_j D_j f_j^{eq} - \sum_j \mathbf{c}_j G_j + \mathcal{O}(\Delta t) \right). \quad (2.18)$$

Then substituting Eqs. (2.9) into Eq. (2.18), we can obtain

$$\begin{aligned} \sum_j \mathbf{c}_j f_j^{ne} &= -\tau \Delta t \left(\partial_t \left(\sum_j \mathbf{c}_j f_j^{eq} \right) + \nabla \cdot \sum_j \mathbf{c}_j \mathbf{c}_j f_j^{eq} \right) + \mathcal{O}(\Delta t^2) \\ &= -\tau \Delta t c_s^2 \nabla \phi + \mathcal{O}(\Delta t^2). \end{aligned} \quad (2.19)$$

With the aid of Eq. (2.19) and taking $\alpha = (\tau - \frac{1}{2})c_s^2\Delta t$, Eqs. (2.17b) can be rewritten as

$$\partial_t \phi = \nabla \cdot (\alpha \nabla \phi) + G + \mathcal{O}(\Delta t^2).$$

From the above discussion, it is clear that the diffusion equation (2.5) can be recovered with second-order accuracy in the time step.

3 Numerical simulation

In this section, some numerical experiments are carried out to test our model. In all simulations, $\gamma = 0$ in our LB model, and the non-equilibrium extrapolation scheme proposed by Guo et al. [28] is used to treat the boundary conditions unless otherwise stated. The global relative error (GRE) used in this paper is as follows,

$$GRE = \frac{\sum_j |\rho(\mathbf{x}_j, t) - \rho^*(\mathbf{x}_j, t)|}{\sum_j |\rho^*(\mathbf{x}_j, t)|}, \quad (3.1)$$

where $\rho(\mathbf{x}_j, t)$ and $\rho^*(\mathbf{x}_j, t)$ are the numerical and analytical solutions, respectively. The summation is taken over all grid points.

3.1 Example 1

We first consider the following one-dimensional CDE

$$\frac{\partial \rho}{\partial t} + u \frac{\partial \rho}{\partial x} = \alpha \frac{\partial^2 \rho}{\partial x^2}, \quad x \in [0, 2]. \quad (3.2)$$

The initial and boundary conditions are determined by the following analytical solution,

$$\rho = e^{-\pi^2 \alpha t} [\cos(\pi x) \cos(\pi u t) + \sin(\pi x) \sin(\pi u t)]. \quad (3.3)$$

From the discussion in Section 2, the exponential transformation

$$\rho(x, t) = \phi(x, t) \exp\left(\frac{u}{2\alpha}x - \frac{u^2}{4\alpha}t\right)$$

can be used to convert Eq. (3.2) into the following diffusion equation,

$$\frac{\partial \phi}{\partial t} = \alpha \frac{\partial^2 \phi}{\partial x^2}. \quad (3.4)$$

Then, the initial and boundary conditions of Eq. (3.3) can be given by

$$\phi(x, t) = \exp\left(-\frac{ux}{2\alpha} + \frac{u^2}{4\alpha}t\right) e^{-\pi^2 \alpha t} [\cos(\pi x) \cos(\pi u t) + \sin(\pi x) \sin(\pi u t)]. \quad (3.5)$$

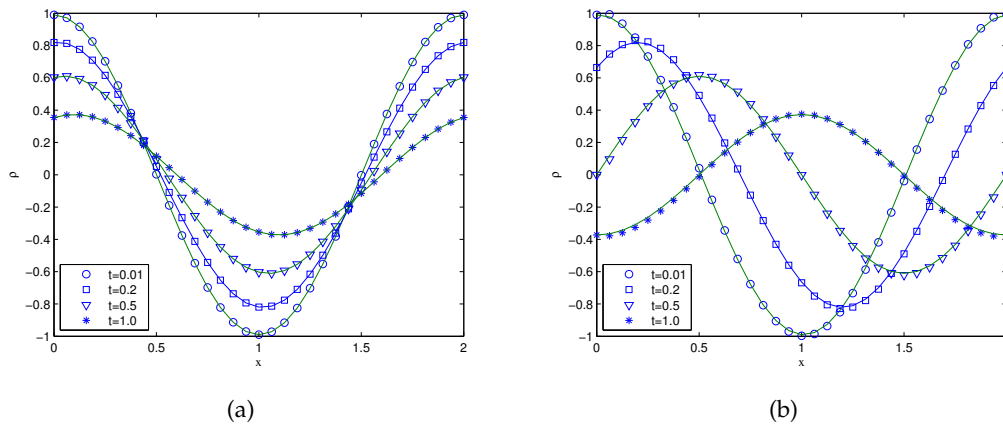


Figure 1: Numerical and analytical solutions at different times for Example 1 ((a) $u=0.1, \alpha=0.1$, (b) $u=1.0, \alpha=0.1$; solid lines: analytical results, symbols: numerical results).

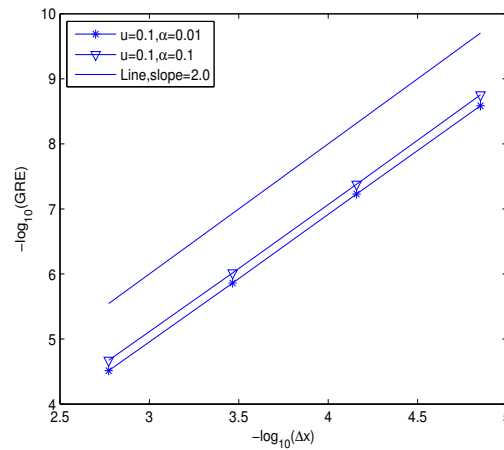


Figure 2: GRES of the present LB model for Example 1 at $t=1.0$, the slope of the inserted line is 2.0, which indicates the present LB model has second-order convergence rate.

In our simulations, $\Delta x=2/32$, $\Delta t=0.001$, the D1Q3 lattice model is used, and the free parameter of the equilibrium distribution function is $a=\frac{1}{6}$. Fig. 1 shows the numerical and analytical solutions at different times for $u=0.1, \alpha=0.1$ and $u=1.0, \alpha=0.1$. From this figure, we can find that the numerical results are in good agreement with the corresponding analytical solutions.

To test the convergence rate of the present model, we carry out some simulations under different Δx : $2/32$, $2/64$, $2/128$, and $2/256$, corresponding to $\Delta t=0.01$, 0.0025 , 0.000625 and 0.00015625 . Fig. 2 shows the GRES for $u=0.1, \alpha=0.01$ and $u=0.1, \alpha=0.1$ at $t=1.0$. It can be seen from Fig.2 that the slopes of the fitting lines for different results

are very close to 2, which indicates that the present model has second-order convergence rate in space.

3.2 Example 2

In this example, we will consider the following two-dimensional CDE

$$\frac{\partial \rho}{\partial t} + u \left(\frac{\partial \rho}{\partial x} + \frac{\partial \rho}{\partial y} \right) = \alpha \left(\frac{\partial^2 \rho}{\partial x^2} + \frac{\partial^2 \rho}{\partial y^2} \right), \quad (x, y) \in [0, l_x] \times [0, l_y], \quad (3.6)$$

with the initial condition

$$\rho(x, y, 0) = \rho_0 e^{\frac{u}{2\alpha}(x+y)} \sin\left(\frac{\pi x}{l_x}\right) \sin\left(\frac{\pi y}{l_y}\right), \quad (3.7)$$

and the boundary conditions

$$\rho(x, 0, t) = \rho(x, l_y, t) = \rho(0, y, t) = \rho(l_x, y, t) = 0. \quad (3.8)$$

The analytical solution of the problem can be given as

$$\rho(x, y, t) = \rho_0 e^{-(b_x + b_y)t + \frac{u}{2\alpha}(x+y)} \sin\left(\frac{\pi x}{l_x}\right) \sin\left(\frac{\pi y}{l_y}\right), \quad (3.9)$$

where

$$b_x = \left[4 \left(\frac{\pi}{l_x} \right)^2 + \left(\frac{u}{\alpha} \right)^2 \right] \cdot \frac{\alpha}{4}, \quad b_y = \left[4 \left(\frac{\pi}{l_y} \right)^2 + \left(\frac{u}{\alpha} \right)^2 \right] \cdot \frac{\alpha}{4}.$$

In our simulations, $l_x = l_y = 1.0$, $\rho_0 = 1.0$.

Here we compare the present LB model with the other two LB models (model 1 and model 2), which are proposed by Shi et al. [19] and Chopard et al. [29], respectively. In our LB model the free parameter is $a = \frac{1}{6}$, which means that, the D2Q5 LB model is adopted. The quadratic equilibrium distribution function is applied in model 1, and we use the D2Q9 lattice model to solve the CDE. However, the linear equilibrium distribution function and auxiliary source term are applied in model 2, and the D2Q5 lattice model is used to solve the CDE. It should be mentioned that, the term $\partial_t(\rho \mathbf{u})$ in the auxiliary source term of model 2 is calculated by the analytical solution. If we use the first-order explicit difference scheme to compute the term $\partial_t(\rho \mathbf{u})$, it will take a longer computational time.

The global relative errors and computational times T_c of the three models at 1000 time steps are presented in Table 1, where the lattice size is 256×256 , $\Delta t = 0.001$. From Table 1, we can find that the GREs of the present LB model are smaller than those of the other two models, especially as the velocity u is large.

In Table 1, the parameter η_1 represents the computational time ratio of the present LB model to the model 1, and η_2 represents the computational time ratio of the present LB model to the model 2. It can be found that η_1 and η_2 are about 36% and 14% respectively.

Table 1: GREs and computational times T_c of the three LB models for Example 2 ($t=1.0$).

u	α	present		model 1			model 2		
		GRE	T_c	GRE	T_c	η_1	GRE	T_c	η_2
0.001	0.001	2.131×10^{-5}	5.9	2.482×10^{-5}	16.1	37%	2.442×10^{-5}	40.9	14%
	0.01	3.246×10^{-4}	5.9	4.286×10^{-4}	16.2	36%	3.248×10^{-4}	42.4	14%
	0.1	6.773×10^{-4}	5.9	9.801×10^{-2}	16.3	36%	6.772×10^{-4}	42.0	14%
0.01	0.001	2.142×10^{-5}	6.0	1.566×10^{-4}	16.1	37%	1.517×10^{-4}	42.3	14%
	0.01	3.246×10^{-4}	5.9	4.484×10^{-4}	16.1	37%	3.450×10^{-4}	42.3	14%
	0.1	6.773×10^{-4}	5.9	9.795×10^{-2}	16.3	36%	6.687×10^{-4}	42.4	14%
0.1	0.001	2.594×10^{-5}	5.9	1.569×10^{-2}	16.3	36%	1.443×10^{-2}	41.0	14%
	0.01	3.242×10^{-4}	5.9	1.476×10^{-3}	16.1	37%	1.518×10^{-3}	41.3	14%
	0.1	6.765×10^{-4}	5.8	9.178×10^{-2}	16.6	35%	9.736×10^{-4}	40.7	14%
1	0.01	3.140×10^{-4}	5.7	6.797×10^{-1}	16.2	35%	4.178×10^{-1}	41.8	14%
	0.1	6.445×10^{-4}	6.0	3.536×10^{-1}	16.3	37%	1.109×10^{-1}	41.1	15%

Table 2: GREs of the three LB models for Example 2 ($u > c$).

Δt	c	u	α	present	model 1	model 2
0.001	2.5	3	0.1	3.6429×10^{-3}	—	—
			0.01	6.6937×10^{-4}	—	—
0.01	0.25	0.5	0.01	8.1544×10^{-2}	—	—
			0.001	$6.8510e \times 10^{-4}$	—	—

It shows that our LB model is more effective than the other two models. This result is expected because our model uses a simpler equilibrium distribution function.

According to the study of Ginzburg [30], the LBM for CDE is stable only under the condition of $|\mathbf{u}/c_s|^2 \leq 1$. While such condition is always satisfied in the LBM for DE, because of the absence of the convection term. To show the advantage of the present LB model, some simulations are conducted with $u > c$ in which the lattice size is 400×400 , $\Delta t = 0.001$ to 0.1 , and c is correspondingly changed from 2.5 to 0.25 . As shown in Table 2, it can be found that the present LB model also works well even as $u > c$, while the other two LB models are unstable.

3.3 Example 3

To further test the present LB model, another two-dimensional CDE with a source term is studied

$$\frac{\partial \rho}{\partial t} + u_1 \frac{\partial \rho}{\partial x} + u_2 \frac{\partial \rho}{\partial y} = \frac{1}{Pe} \left(\frac{\partial^2 \rho}{\partial x^2} + \frac{\partial^2 \rho}{\partial y^2} \right) + F(\mathbf{x}, t), \quad \mathbf{x} = (x, y) \in [0, 2] \times [0, 2], \quad (3.10)$$

where

$$F(x, y; t) = \exp \left(\left(1 - \frac{2\pi^2}{Pe} \right) t \right) (\pi(u_1 + u_2) \cos(\pi(x + y)) + \sin(\pi(x + y))). \quad (3.11)$$

Table 3: GREs of the three LB models for Example 3 ($t=1.0$).

u	Pe	present	model 1	model 2
0.01	10	2.678×10^{-3}	1.431×10^{-2}	2.691×10^{-3}
	100	6.459×10^{-5}	5.790×10^{-5}	6.311×10^{-5}
	1000	3.946×10^{-4}	1.134×10^{-4}	1.121×10^{-4}
0.1	10	2.777×10^{-3}	1.415×10^{-2}	3.874×10^{-3}
	100	1.033×10^{-3}	2.923×10^{-4}	1.402×10^{-4}
1.0	10	1.828×10^{-2}	9.149×10^{-3}	3.158×10^{-2}
	100	9.729×10^{-2}	9.877×10^{-5}	2.961×10^{-3}

The problem has the following analytical solution

$$\rho(x,y;t) = \exp\left(\left(1 - \frac{2\pi^2}{Pe}\right)t\right) \sin(\pi(x+y)). \quad (3.12)$$

The initial and boundary conditions are determined by the analytical solution.

In the simulations, $\Delta x = 2/256$, $\Delta t = 0.001$, $u_1 = u_2 = u$. Similar to Example 2, the GREs at $t=1.0$ for the three different LB models are also calculated and shown in Table 3. From this table, we can observe that the GREs of the three models are not very different.

To test the convergence rate of the present LB model, we carry out some simulations under different lattice sizes: 32×32 , 64×64 , 128×128 , and 256×256 , corresponding to $\Delta t = 0.01$, 0.0025 , 0.000625 and 0.00015625 . The GREs of the cases with $u_1 = u_2 = 0.01$, $Pe = 10, 100$ and 1000 are calculated and presented in Fig. 3. From this figure, we can find that the present LB model has second-order accuracy in space.

3.4 Example 4

Then, the following three-dimensional CDE with a source term

$$\begin{aligned} & \frac{\partial \rho}{\partial t} + u_1 \frac{\partial \rho}{\partial x} + u_2 \frac{\partial \rho}{\partial y} + u_3 \frac{\partial \rho}{\partial z} \\ &= \frac{1}{Pe} \left(\frac{\partial^2 \rho}{\partial x^2} + \frac{\partial^2 \rho}{\partial y^2} + \frac{\partial^2 \rho}{\partial z^2} \right) + F(\mathbf{x}, t), \quad \mathbf{x} = (x, y, z) \in [0, 2] \times [0, 2] \times [0, 2], \end{aligned} \quad (3.13)$$

is also studied to test the present LB model, where

$$\begin{aligned} & F(x, y, z; t) \\ &= \exp\left(\left(1 - \frac{3\pi^2}{Pe}\right)t\right) (\pi(u_1 + u_2 + u_3) \cos(\pi(x+y+z)) + \sin(\pi(x+y+z))). \end{aligned} \quad (3.14)$$

The analytical solution of the problem is as follow

$$\rho(x, y, z; t) = \exp\left(\left(1 - \frac{3\pi^2}{Pe}\right)t\right) \sin(\pi(x+y+z)). \quad (3.15)$$

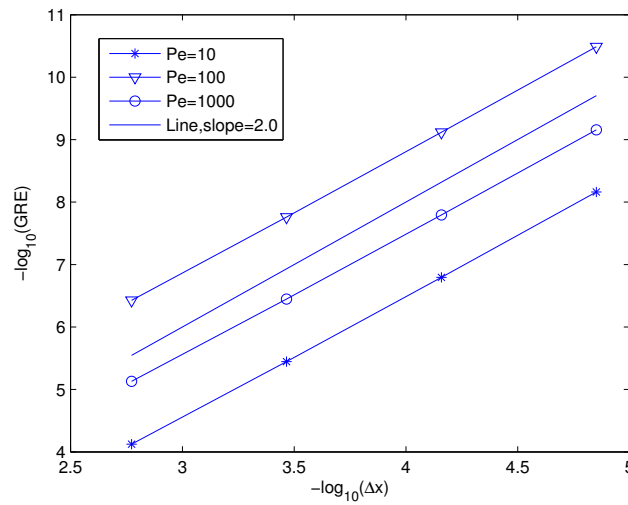


Figure 3: GREs of the present LB model for Example 3 at $t=1.0$, the slope of the inserted line is 2.0, which indicates the present LB model has second-order convergence rate.

The initial and boundary conditions are determined by the analytical solution.

Similar to Example 2 and Example 3, we also compare the present LB model with the other two LB models (model 1 and model 2). In our LB model, the free parameter of the equilibrium distribution function is $a = \frac{1}{6}$, and the D3Q7 lattice model is used. In model 1, we use the D3Q15 lattice model to solve the 3D CDE. However, the D3Q7 lattice model is used in model 2. In the simulations, the lattice size is $100 \times 100 \times 100$, and $\Delta t = 0.001$, $u_1 = u_2 = u_3 = u$.

The GREs at $t = 1.0$ for the three different LB models are calculated and shown in Table 4. From this table, we can observe that the GREs of the three models are not very different except the case with $u = 1.0$ and $Pe = 100$, in which the transformation of our model reaches up to e^{150} and leads to an instability problem.

To test the convergence rate of the present LB model, we carry out some simulations under different lattice sizes: $20 \times 20 \times 20$, $40 \times 40 \times 40$, $80 \times 80 \times 80$, and $100 \times 100 \times 100$, corresponding to $\Delta t = 0.01$, 0.0025 , 0.000625 and 0.0004 . The GREs of the cases with $u = 0.01$, $Pe = 10$ and 100 are calculated and presented in Fig. 4. From this figure, we can find that the present LB model has second-order accuracy in space.

3.5 Example 5

Finally, to demonstrate the applicability of the present LB model for problems in irregular domains, a convection-diffusion problem in an isosceles trapezoidal region is studied.

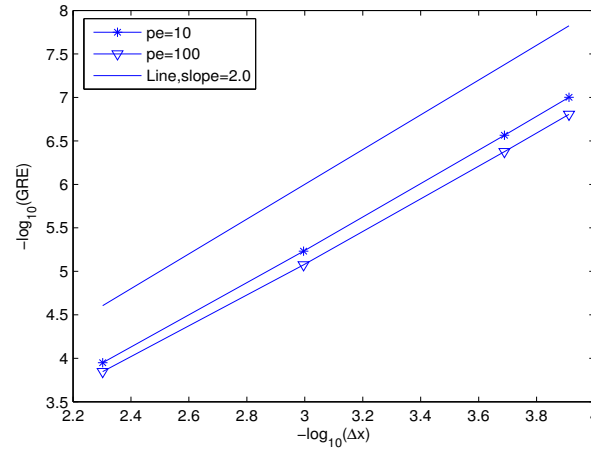


Figure 4: GREs of the present LB model for Example 4 at $t=1.0$, the slope of the inserted line is 2.0, which indicates the present LB model has second-order convergence rate.

The CDE for this problem can be written as

$$\frac{\partial \rho}{\partial t} + u \left(\frac{\partial \rho}{\partial x} + \frac{\partial \rho}{\partial y} \right) = \alpha \left(\frac{\partial^2 \rho}{\partial x^2} + \frac{\partial^2 \rho}{\partial y^2} \right), \quad (x, y) \in \Omega, \quad (3.16)$$

where Ω is the isosceles trapezoidal region as shown in Fig. 5. The skewed angle between the top and right boundaries is set to be $\theta=60$. L is the length of the top boundary of the isosceles trapezoidal region, H is the height of the region.

The initial and boundary conditions are determined by the following analytical solution of the problem

$$\rho = \frac{1}{\pi(10+4\alpha t)} \exp \left(-\frac{(x-ut)^2 + (y-ut)^2}{10+4\alpha t} \right). \quad (3.17)$$

In our simulations, L and H are set to be 1 and $\sqrt{3}/3$, and a 444×256 lattice is used. The non-equilibrium extrapolation scheme proposed by Guo et al. [28] is used to treat the

Table 4: GREs of the three LB models for Example 4 ($t=1.0$).

u	Pe	present	model 1	model 2
0.01	10	1.932×10^{-3}	1.804×10^{-3}	1.933×10^{-3}
	100	1.106×10^{-3}	1.269×10^{-3}	1.077×10^{-3}
	1000	3.545×10^{-3}	1.024×10^{-3}	9.891×10^{-4}
0.1	10	2.095×10^{-3}	1.763×10^{-3}	2.109×10^{-3}
	100	4.089×10^{-3}	1.270×10^{-3}	9.994×10^{-4}
1.0	10	9.695×10^{-3}	1.040×10^{-3}	7.482×10^{-3}
	100	—	1.125×10^{-3}	8.219×10^{-4}

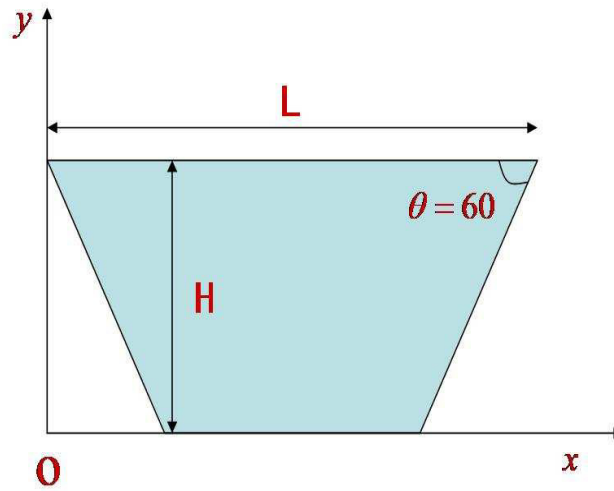
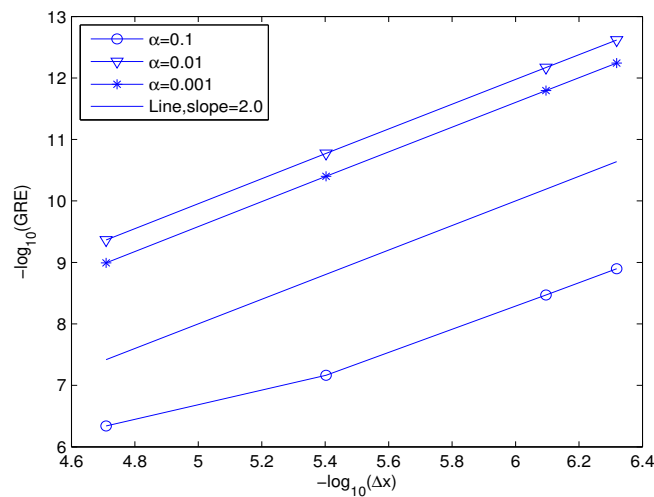


Figure 5: Coordinate of the isosceles trapezoidal region.

Figure 6: GREs of the present LB model for Example 5 at $t = 1.0$, the slope of the inserted line is 2.0, which indicates the present LB model has second-order convergence rate.

top and bottom boundaries. While the single-node scheme proposed by Zhang et al. [31] is used to treat the curved boundaries, i.e., the left and right boundaries.

Similar to Example 2, as $t = 1.0$, the GREs at different velocities and diffusion coefficients for the three different LB models are calculated and shown in Table 5. From this table, we can find that the GREs of the three models are not very different.

Table 5: GREs of the three LB models for Example 5 ($t=1.0$).

u	α	present	model 1	model 2
0.001	0.001	1.137×10^{-7}	1.117×10^{-7}	8.400×10^{-8}
	0.01	1.413×10^{-5}	1.824×10^{-5}	1.478×10^{-5}
	0.1	5.004×10^{-4}	7.789×10^{-4}	5.006×10^{-4}
0.01	0.001	1.661×10^{-5}	7.584×10^{-6}	2.924×10^{-7}
	0.01	1.196×10^{-5}	1.728×10^{-5}	1.247×10^{-5}
	0.1	4.761×10^{-4}	7.436×10^{-4}	4.874×10^{-4}
0.1	0.001	7.323×10^{-3}	1.923×10^{-3}	2.502×10^{-6}
	0.01	2.402×10^{-3}	2.538×10^{-3}	1.532×10^{-5}
	0.1	3.444×10^{-4}	1.331×10^{-3}	3.670×10^{-4}
1.0	0.001	9.551×10^{-1}	2.738×10^{-1}	2.363×10^{-4}
	0.01	6.545×10^{-1}	2.782×10^{-1}	$2.128 \times 10^{+2}$

To test the convergence rate of the present LB model, we carry out some simulations under different lattice sizes: 111×64 , 222×128 , 444×256 and 555×320 , corresponding to $\Delta t = 0.01$, 0.0025 , 0.000625 and 0.0004 . The GREs of the cases with $u = 0.01$, $\alpha = 0.1$, 0.01 and 0.001 are calculated and presented in Fig. 6. From this figure, we can find that the present LB model also has second-order accuracy in space for the convection-diffusion problem in irregular domain.

4 Conclusions

In this paper, an exponential transformation based LB model is proposed for the n D CDE. In order to eliminate the convection term, an exponential transformation is introduced to convert the n D CDE into a DE. Then, when we use the LB model to solve the converted DE, the simpler linear equilibrium distribution function and fewer discrete velocities can be chosen. Because of that, compared to the existing LBMs for CDE, the computation efficiency and stability of the present LB model for CDE are improved.

To confirm the accuracy and effectiveness of the present LB model, five numerical examples are carried out. The results show that the present LB model has second-order convergence rate in space. Besides that, compared to the LB models for CDE in [19, 29], the present LB model is more efficient and the accuracy is also competitive to some extent. Furthermore, we can find that the present LB model is also more stable and works well even when $u > c$.

In the future, we will attempt to eliminate the instability caused by the overlarge transformation coefficient. In addition, the exponential transformation based LB model will be extended to solve the nonlinear CDE.

Acknowledgements

This work is financially supported by the National Natural Science Foundation of China (Grant Nos. 12072127 and 11702259) and the Guidance Project of Scientific Research Program of Hubei Provincial Department of Education (Grant No. B2021322).

References

- [1] F. TONG, X. FENG AND Z. LI, *Fourth order compact FD methods for convection diffusion equations with variable coefficients*, Appl. Math. Lett., 121 (2021), 107413.
- [2] H. ALI, M. KAMRUJJAMAN AND M. S. ISLAM, *Numerical computation of FitzHugh-Nagumo equation: A novel Galerkin finite element approach*, Int. J. Math. Res., 9(1) (2020), pp. 20–27.
- [3] S. A. LIMA, M. KAMRUJJAMAN AND M. S. ISLAM, *Direct approach to compute a class of reaction-diffusion equation by a finite element method*, J. Appl. Math. Comput., 4(2) (2020), pp. 26–33.
- [4] B. R. BALIGAA AND S. V. PATANKA, *A new finite-element formulation for convection-diffusion problems*, Numer. Heat Transf., 3(4) (1980), pp. 393–409.
- [5] O. ANGELINI, K. BRENNER AND D. HILHORST, *A finite volume method on general meshes for a degenerate parabolic convection-reaction-diffusion equation*, Numer. Math., 123(2) (2013), pp. 219–257.
- [6] X. X. YUE, F. J. WANG, Q. S. HUA AND X. Y. QIU, *A novel space-time meshless method for nonhomogeneous convection-diffusion equation with variable coefficients*, Appl. Math. Lett., 92 (2019), pp. 144–150.
- [7] C. X. ZHANG, C. WANG, S. H. CHEN AND F. J. WANG, *A novel localied meshless method for solving transient heat conduction problems in complicated domains*, Comput. Modeling Eng. Sci., 135(3) (2023), pp. 2407–2424.
- [8] F. J. WANG, C. M. FAN, C. Z. ZHANG AND J. LIN, *A localized space-time method of fundamental solutions for diffusion and convection-diffusion problems*, Adv. Appl. Math. Mech., 12(4) (2020), pp. 940–958.
- [9] Y. H. QIAN, S. SUCCI AND S. A. ORSZAG, *Recent advances in lattice Boltzmann computing*, Annu. Rev. Comput. Phys., III (1995), pp. 195–242.
- [10] R. BENZI, S. SUCCI AND M. VERGASSOLA, *The lattice Boltzmann equation: theory and applications*, Phys. Rep., 222(3) (1992), pp. 145–197.
- [11] S. CHEN AND G. D. DOOLEN, *Lattice Boltzmann method for fluid flows*, Annu. Rev. Fluid Mech., 30(1) (1998), pp. 329–364.
- [12] C. K. AIDUN AND J. R. CLAUSEN, *Lattice-Boltzmann method for complex flows*, Annu. Rev. Fluid Mech., 42 (2010), pp. 439–472.
- [13] S. SUCCI, *The Lattice Boltzmann Equation for Fluid Dynamics and Beyond*, Oxford University Press, 2001.
- [14] Z. H. CHAI AND B. C. SHI, *A novel lattice Boltzmann model for the Poisson equation*, Appl. Math. Model., 32(10) (2008), pp. 2050–2058.
- [15] J. ZHANG, G. YAN AND Y. DONG, *A new lattice Boltzmann model for the Laplace equation*, Appl. Math. Comput., 215 (2009), pp. 539–547.
- [16] Q. H. LI, Z. H. CHAI AND B. C. SHI, *Lattice Boltzmann models for two-dimensional coupled Burgers' equations*, Comput. Math. Appl., 75 (2018), pp. 864–875.

- [17] X. T. QI, B. C. SHI AND Z. H. CHAI, *Cole-Hopf transformation based lattice Boltzmann model for one-dimensional Burgers' equation*, *Commun. Theor. Phys.*, 69 (2018), pp. 329–335.
- [18] S. P. DAWSON, S. CHEN AND G. D. DOOLEN, *Lattice Boltzmann computations for reaction-diffusion equations*, *J. Chem. Phys.*, 98 (1993), pp. 1514–1523.
- [19] B. C. SHI, B. DENG, R. DU AND X. W. CHEN, *A new scheme for source term in LBGK model for convection-diffusion equation*, *Comput. Math. Appl.*, 55(7) (2008), pp. 1568–1575.
- [20] B. C. SHI AND Z. L. GUO, *Lattice Boltzmann model for nonlinear convection-diffusion equations*, *Phys. Rev. E*, 79 (2009), 016701.
- [21] Z. H. CHAI AND T. S. ZHAO, *Lattice Boltzmann model for the convection-diffusion equation*, *Phys. Rev. E*, 87 (2013), 063309.
- [22] H. YOSHIDA AND M. NAGAOKA, *Multiple-relaxation-time lattice Boltzmann model for the convection and anisotropic diffusion equation*, *J. Comput. Phys.*, 229 (2010), pp. 7774–7795.
- [23] L. WANG, B. C. SHI AND Z. H. CHAI, *Regularized lattice Boltzmann model for a class of convection-diffusion equations*, *Phys. Rev. E*, 92 (2015), 043311.
- [24] L. LI, R. W. MEI AND J. F. KLAUSNER, *Lattice Boltzmann models for the convection-diffusion equation: D2Q5 vs D2Q9*, *Int. J. Heat Mass Transf.*, 108 (2017), pp. 41–62.
- [25] Z. H. CHAI AND B. C. SHI, *Multiple-relaxation-time lattice Boltzmann method for the Navier-Stokes and nonlinear convection-diffusion equations: Modeling, analysis, and elements*, *Phys. Rev. E*, 102(2) (2020), 023306.
- [26] H. BRENNER, *The diffusion model of longitudinal mixing in beds of finite length. Numerical values*, *Chem. Eng. J.*, 17(4) (1962), pp. 229–243.
- [27] Q. F. ZHANG AND C. J. ZHANG, *A new linearized compact multisplitting scheme for the nonlinear convection-rection-diffusion equations with delay*, *Commun. Nonlinear Sci. Numer. Simul.*, 18(12) (2013), pp. 3278–3288.
- [28] Z. L. GUO, C. G. ZHENG AND B. C. SHI, *Non-equilibrium extrapolation method for velocity and pressure boundary conditions in the lattice Boltzmann method*, *Chinese Phys.*, 11 (2002), pp. 366–374.
- [29] B. CHOPARD, J. L. FALCONE AND J. LATT, *The lattice Boltzmann advection-diffusion model revisited*, *Euro. Phys. J. Special Topics*, 171(1) (2009), pp. 245–249.
- [30] I. GINZBURG, *Truncation errors, exact and heuristic stability analysis of two-relaxation-times lattice Boltzmann schemes for anisotropic advection-diffusion equation*, *Commun. Comput. Phys.*, 11 (2012), pp. 1439–1502.
- [31] M. X. ZHANG, W. F. ZHAO, AND P. LIN, *Lattice Boltzmann method for general convection-diffusion equations: MRT model and boundary schemes*, *J. Comput. Phys.*, 389 (2019), pp. 147–163.